Original Article
Oxysophocarpine inhibits lung injury induced by respiratory syncytial virus

Jie Gao, Ying Li, Qiwei Wang, Xiaojian Ma, Yan Zhang

Department of Pediatrics, Henan University Huaihe Hospital, Kaifeng 475000, Henan, P. R. China

Abstract: Oxysophocarpine (OSC) has various pharmacological effects. This study was designed to investigate whether OSC confers protection against respiratory syncytial virus (RSV) infection-induced lung injury. Here, we found that OSC inhibited RSV replication and increased the viability of RSV-infected lung epithelial A549 cells. OSC suppressed the RSV-increased production and release of pro-inflammatory cytokines and chemokines [tumor necrosis factor-α, interleukin-6 (IL-6), IL-8, regulated on activation in normal T-cell expressed and secreted, macrophage inflammatory protein-1α; and monocyte chemoattractant protein-1] in A549 cells. OSC also reduced the formation of reactive oxygen species and enhanced the activities of antioxidant enzymes in RSV-infected cells. The anti-oxidative effect of OSC on RSV-infected cells was dependent on NF-E2-related factor 2 activation. In vivo, OSC significantly alleviated RSV-triggered mouse lung injury. Overall, these results indicated that OSC attenuates RSV-enhanced pulmonary damage by inhibiting oxidative stress and inflammation.

Keywords: Oxysophocarpine, respiratory syncytial virus, NF-E2-related factor 2, inflammation, oxidative stress

Introduction

Respiratory syncytial virus (RSV) is a non-segmented, negative-sense, single-stranded RNA virus belonging to the *Paramyxoviridae* family. RSV is the leading cause of severe lower respiratory tract infections in children as well as in elderly and immune-suppressed individuals worldwide [1, 2]. Despite the significant impact of RSV infection-mediated lung injury on patient's morbidity and mortality, treatment options remain largely limited [3]. Therefore, exploring effective and safe drugs to treat RSV-induced airway diseases is very important and urgent.

Extensive inflammation plays an essential role in RSV-leading airway damage. Following RSV infection, airway epithelial cells produce a variety of immunologically active molecules, such as cytokines, chemokines, and adhesion molecules [4]. Oxidative stress also contributes to pathogenesis of both acute and chronic lung inflammatory diseases, such as asthma, fibrosis, and chronic obstructive pulmonary disease [5-7]. Reactive oxygen species (ROS) is highly involved in RSV-enhanced lung epithelial cell

activation [8, 9]. RSV infection induces ROS formation, which triggers the expression of pro-inflammatory molecules, such as tumor necrosis factor-α (TNF-α), interleukin (IL)-6, IL-8, regulated on activation in normal T-cell expressed and secreted (RANTES)/CCL5, macrophage inflammatory protein-1α (MIP-1α)/CCL3, and monocyte chemoattractant protein-1 (MCP-1) [6, 7]. A previous study has established that RSV-mediated inhibition of antioxidant enzymes (AOEs) contributes to the pathogenesis of severe bronchiolitis [9]. AOEs, such as superoxide dismutase (SOD), catalase (CAT), glutathione peroxidase (GPx), and glutathione S-transferase (GST), can either directly decompose ROS (e.g., SOD and CAT) or facilitate their antioxidant reactions (e.g., GPx) [10]. Transcriptional activation of AOEs mainly occurs through binding of NF-E2-related factor 2 (Nrf2) to the *cis*-acting antioxidant response elements (AREs) [10]. This element has been identified in the regulatory regions of genes encoding many AOEs, including SOD, CAT, hemeoxygenase 1, and GST [11]. The protective role of the Nrf2-ARE pathway has been proven in several experimental models of pulmonary disorders, includ-

Figure 1. The chemical structure of OSC.
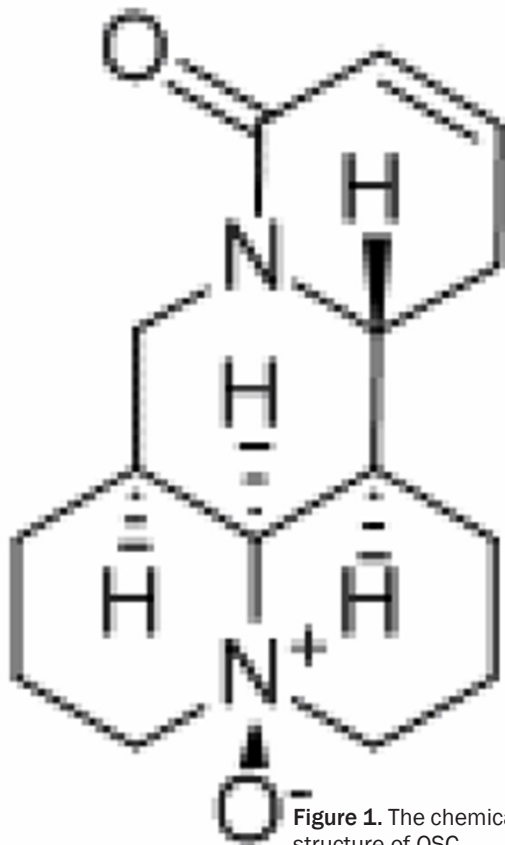
ing RSV-triggered lung injury [12-16]. Thus, targeting of inflammation and oxidative stress is a potential therapeutic strategy for RSV-induced lung damage.

Oxysophocarpine (OSC, **Figure 1**) is a quinolizidine alkaloid extracted from *Sophora flavescens* Ait., *S. alopecuroides* Linn., and other leguminous plants of *Robinia*. OSC has been utilized as traditional Chinese medicine owing to its neuroprotective, cardioprotective, analgesic, anti-inflammatory, anti-tumor, anti-nociceptive, and anti-viral activities [17-20]. OSC possessed significant anti-HBV activity, showing inhibitory potency against HBsAg secretion [21], and also reduced the mortality of enterovirus 71-infected mice [22]. However, whether OSC exerts protective effects against RSV-initiated pulmonary injury is unclear.

This study evaluated the protective effects of OSC on RSV-infected A549 cells and mouse lungs. We found that OSC reduced the RSV-decreased cell viability, replication of RSV, release of pro-inflammatory cytokines and che-

mokines, and production of ROS but enhanced the activities of AOEs in A549 cells. Moreover, the anti-oxidative effect of OSC on RSV-infected cells was dependent on Nrf2 activation. In vivo studies on RSV-infected mice were consistent with in vitro findings. Overall, the results presented here suggest that OSC protects against RSV-induced lung injury by inhibiting inflammatory responses and oxidative stress.

Materials and methods

RSV preparation

The RSV A2 strain was obtained from American Type Culture Collection (ATCC; Manassas, VA, USA), grown in Hep-2 cells (ATCC), and purified through polyethylene glycol precipitation followed by centrifugation on discontinuous sucrose gradients as previously described [23]. The virus titer of the purified RSV pools was 2×10^7 plaque-forming units (PFU)/mL as determined by using methylcellulose plaque assay. Virus pools were aliquoted, quickly frozen, and stored at -80°C before use. Sucrose-purified extracts from uninfected Hep-2 cells were also generated under the same conditions.

Cell culture and treatment

A549 cell (ATCC), a human alveolar type II-like epithelial cell line, was cultured in F12K medium (AppliChem, Darmstadt, Germany) containing 10% fetal bovine serum (FBS; Gibco, BRL, UK), 10 mM glutamine, 100 IU/mL penicillin, and 100 mg/mL streptomycin (all from Sigma-Aldrich, St. Louis, MO, USA). At approximately 80% to 90% confluence, cell monolayers were infected with RSV at a multiplicity of infection (MOI) of 0.3 for 24 h. For OSC (Zi Jin Hua Pharmaceutical Co., Yinchuan, Ningxia, China) treatment, OSC (0, 1, 2, and 5 μM) was added into the cells and cultured for 1 h prior to RSV infection. The cells with neither RSV infection nor OSC treatment were used as control.

Animal protocols

6- to 8-week-old female BALB/c mice (Laboratory Animal Center of Henan Province, Zhengzhou, Henan, China) were housed in specific pathogen-free conditions under a 12 h light/dark cycle and maintained at 22°C to 24°C. All studies were approved by the Experimental Animal Committee of Henan Uni-

versity. Under light anesthesia, the mice (n = 5/ group) were inoculated intranasally with 2×10^7 PFU of RSV, which was diluted in sterile phosphate-buffered saline (PBS) for a total of 20 μL inoculation volume. To determine the effects of OSC treatment on RSV infection and related pulmonary damage, we administered intraperitoneal injection of OSC, prepared by dissolving in normal saline, once daily for 7 days at a dose of 80 mg/kg body weight (BW) prior to RSV infection. The mice with neither RSV infection nor OSC treatment were used as control. For all mice, BW was recorded daily before and after RSV challenge.

Sample collection

All of the mice were anesthetized and sacrificed 5 days after RSV infection. The lower lobe of the right lung was ligated prior to bronchoalveolar lavage (BAL) and harvested for Western blot and histopathological analyses. BAL was performed as previously described [24]. Briefly, after anesthetization, the trachea was exposed and cannulated with a 22-G intravenous cannula. PBS (0.8 mL) was injected and withdrawn for the first lavage. The lavage procedure was performed thrice. BAL fluid (BALF) samples were centrifuged at 1000 × *g* for 8 min at 4°C and subsequently stored at -80°C for the subsequent experiments.

Lung histopathology

The lung tissue was fixed in 10% formalin for 24 h, embedded in paraffin, cut into 4 μm-thick sections, and stained with hematoxylin and eosin (H&E, Sigma). The tissues were subsequently mounted and covered with coverslips using Dako-mounting medium (Dakocytomation, Denmark, CA, USA). The infiltration degree of airway inflammatory cells was scored in a double-blind screening by two independent pathologists. Peribronchiole and perivascular inflammation were evaluated using a scoring system of 0-4, where 0 represents no cells; 1 indicates few cells; 2 indicates a ring of inflammatory cells 1 cell layer deep; 3 indicates a ring of inflammatory cells 2-4 cell layers deep; and 4 indicates a ring of inflammatory cells > 4 cell layers deep.

Lung wet/dry (W/D) weight ratio

Mice were sacrificed 5 days after RSV infection. After being harvested, the lungs were weighed,

dehydrated at 80°C for 24 h, and then weighed again when dried. The severity of pulmonary edema was measured using the lung W/D weight ratio.

Cell viability assay

Cell viability was determined using the 3-(4,5-dimethylthiazol-2-yl)-2,5-diphenyltetrazolium bromide (MTT; Sigma) assay. Briefly, 24 h after RSV infection, MTT (20 μL; 5 mg/mL) was added into the cell plate and then incubated for 4 h. The medium was subsequently removed, and the cells were dissolved in dimethyl sulfoxide (150 μL) at 37°C for 30 min. The formation of formazan was measured spectrophotometrically at 490 nm using an enzyme-linked immunosorbent assay (ELISA) reader (EL × 800 uv, Bio Tek Instruments, Winooski, VT, USA). Cell viability was expressed as a percentage of the control cells without RSV infection.

Viral titer

Viral titers in the supernatants of the cells and the lung homogenates were measured by using the plaque assay as previously described [25]. Briefly, Hep-2 cells were cultured as monolayers in 24-well plates and then infected with serial 10-fold dilutions of viral suspension in DMEM/F12 (1:1). The overlay was prepared with agar (Sigma-Aldrich) at a final concentration of 1% DMEM/F12: 1% FBS (1:1). After 5 days at 37°C and under 5% CO_2, the plaques were stained with crystal violet and then counted. Viral titers were calculated and expressed as PFU/mL or PFU/g of lung tissue.

ELISAs

To assess the production of cytokines and chemokines, we harvested the supernatants of the cells and the BALFs at indicated time points after infection. The samples were tested for TNF-α, IL-6, IL-8 (KC in mice), RANTES, MIP-1α, and MCP-1 levels by using the commercial ELISA kits obtained from Bio-Rad Laboratories (Hercules, CA, USA) according to the manufacturer's instructions. The absorbance was read at 490 nm on an ELISA plate scanner.

Intracellular ROS measurement

The change in fluorescence resulting from the oxidation of the fluorescent probe 2',7'-dic-
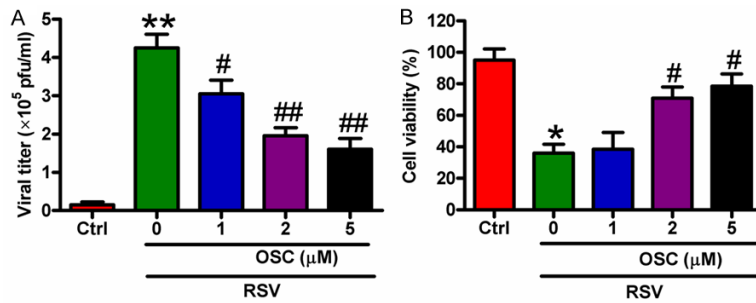
Figure 2. The effect of OSC on RSV replication and RSV-infected A549 cell viability. A549 cells were pretreated with OSC (0, 1, 2, and 5 µM) for 1 h, followed by 0.3 MOI of RSV infection for 24 h. A. RSV replication was measured by using the plaque assay. B. The viability of A549 cells was assessed by MTT assay. Values were presented as mean ± SD of three independent experiments. *P < 0.05, **P < 0.01 vs. Ctrl group; #P < 0.05, ##P < 0.01 vs. RSV alone group.

hlorofluorescein diacetate (DCFH-DA; Nanjing Jiancheng Bioengineering Inst., Nanjing, Jiangsu, China) was used to evaluate the levels of intracellular ROS. Briefly, after RSV or OSC treatment, the cells or the lung homogenates were incubated with 10 µM of DCFH-DA for 30 min at 37°C in the dark. The intensity of fluorescence was detected at an excitation and emission of 485 and 525 nm, respectively, by using a fluorescence microplate reader (Molecular Devices Corp., Sunnyvale, CA, USA).

Measurement of SOD, CAT, GPx, and GST

SOD, CAT, GPx, and GST activities in the supernatants of the cells and the lung homogenates were determined by using specific biochemical assays (Cayman Chemical, Ann Arbor, MI, USA) according to the manufacturer's instructions. SOD activity was determined by using tetrazolium salt to detect superoxide radicals generated by xanthine oxidase and hypoxanthine. One unit of SOD is defined as the amount of enzyme needed to achieve 50% dismutation of the superoxide radical. The SOD activity was expressed as U/mg protein. The CAT activity was quantified based on the reaction of the enzyme with methanol in the presence of an optimal H_2O_2 concentration. The CAT activity was expressed as nM/mg protein. GPx activity was determined through an indirect coupled reaction with glutathione reductase. This method depends on the ability of the enzyme to oxidize GSH, which was monitored by recording the reduction in absorbance of NADPH at 340 nm. The GPx activity was expressed as nM/mg protein. The total GST activity was quantified by measuring the conjugation of 1-chloro-2,4-dinitrobenzene with reduced glutathione. This conjugation is accompanied by an increase in absorbance at 340 nm. And the rate of increase is directly proportional to GST activity, which was expressed as nM/mg protein.

Nrf2 knockdown by siRNA

Two Nrf2 siRNAs (non-overlapping sequences) or negative control (Ctrl) were designed and synthesized by Shanghai Kaiji Biotech. (Shanghai, China), and 100 mM siRNAs or Ctrl were transfected the cells using liposome 2000 (Invitrogen) according to the manufacturer's instruction.

Western blot analysis

Nuclear and cytoplasmic extracts of lung tissues or uninfected or infected A549 cells were prepared using NE-PER Nuclear and Cytoplasmic Extraction Kits (Thermo Scientific, Grand Island, NY, USA). Equal amounts of proteins were separated by electrophoresis on sodium dodecyl sulfate polyacrylamide gel and transferred onto polyvinylidene difluoride membrane (Millipore, Billerica, MA, USA). Nonspecific binding was blocked by immersing the membrane in Tris-buffered saline-Tween 20 (TBST) blocking solution containing 5% non-fat milk powder. After washing in TBST thrice, the membranes were incubated with specific antibodies against Nrf2 (Abcam, Cambridge, UK), SOD, CAT, and GST (all obtained from Santa Cruz Biotechnology, Dallas, TX, USA), as well as anti-lamin B and anti-β-actin (both obtained from Sigma) overnight at 4°C, followed by incubation with the appropriate horseradish-peroxidase-conjugated secondary antibodies diluted in TBST for 1 h at room temperature. Proteins were detected using enhanced-chemiluminescence reagents (Pierce, Rockford, IL, USA). Protein bands were quantified using Quantity One software (BioRad, USA).

Statistical analysis

All data, except for the histopathological scores, are presented as mean ± standard deriva-
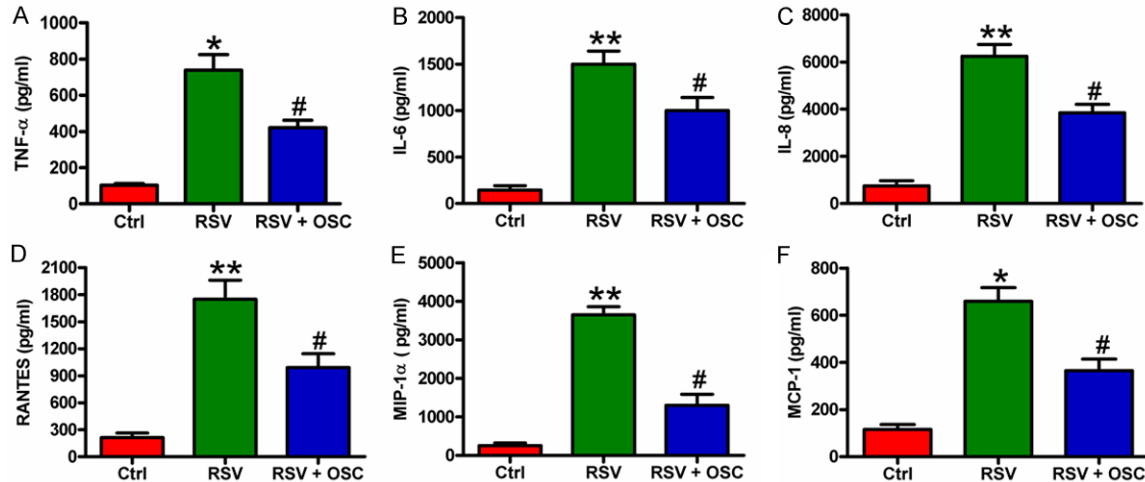
Figure 3. OSC reduced the release of pro-inflammatory cytokines and chemokines in RSV-infected A549 cells. The A549 cells were pretreated with 2 μM of OSC for 1 h followed by 0.3 MOI of RSV infection for 24 h. (A-F) The release of TNF-α (A), IL-6 (B), IL-8 (C), RANTES (D), MIP-1α (E), and MCP-1 (F) in the supernatants of the cells was measured by ELISAs. Values were presented as mean ± SD of three independent experiments. *P < 0.05, **P < 0.01 vs. Ctrl group; #P < 0.05 vs. RSV group.

tion (SD). Histopathological scores were obtained using the nonparametric Kruskal-Wallis method. One-way ANOVA followed by Dunnett's multiple comparison tests was performed to analyze the intergroup differences. All statistical analyses were performed using GraphPad Prism software (ver. 5.0; San Diego, CA, USA). P < 0.05 was considered statistically significant.

Results

OSC inhibits RSV replication and improves RSV-infected A549 cell viability

We first investigated the effect of OSC on RSV replication in A549 cells. We found that OSC inhibited RSV replication in A549 cells in a dose-dependent manner (**Figure 2A**). The effects of OSC on the viability of RSV-infected A549 cells were evaluated by using MTT assay. **Figure 2B** shows that RSV infection significantly reduced the viability of A549 cells. However, this reduction was attenuated by OSC (1, 2, and 5 μM) pretreatment in a dose-dependent manner. Moreover, the pro-survival and anti-viral effects of the two high doses (2 and 5 μM) of OSC showed no significant difference. Therefore, 2 μM of OSC was selected for subsequent experiments. These results indicated that OSC reduces RSV replication and increases RSV-infected A549 cell viability.

OSC reduces RSV-induced production of pro-inflammatory cytokine and chemokine in A549 cells

RSV infection is accompanied by local production of numerous cytokines and chemokines. To analyze the anti-inflammatory effects of OSC on RSV-infected A549 cells, we measured the release of pro-inflammatory cytokines and chemokines in the supernatants of the cells by using ELISAs. We found that RSV-infected A549 cells significantly increased the levels of TNF-α (**Figure 3A**), IL-6 (**Figure 3B**), IL-8 (**Figure 3C**), RANTES (**Figure 3D**), MIP-1α (**Figure 3E**), and MCP-1 (**Figure 3F**) compared with the Ctrl cells. By contrast, OSC attenuated the increase in release of the above-mentioned cytokines and chemokines in RSV-infected A549 cells (**Figure 3A-F**). These data suggested that OSC inhibits the RSV infection-induced production of inflammatory cytokines and chemokines in A549 cells.

OSC inhibits oxidative stress induced by RSV in A549 cells

Oxidative stress is involved in RSV infection and correlated with release of inflammatory mediators from epithelial cells [8]. To investigate whether OSC has an effect on RSV-induced oxidative stress, we determined ROS production and AOE activities in RSV-challenged A549
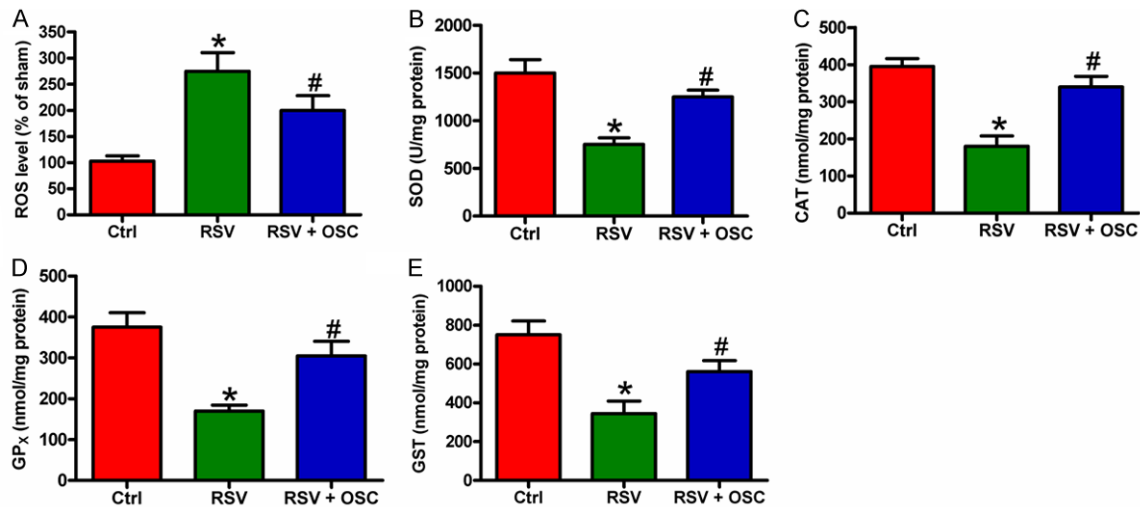
Figure 4. OSC inhibited ROS generation and enhanced AOE activities in RSV-infected A549 cells. A549 cells were pretreated with 2 µM of OSC for 1 h followed by 0.3 MOI of RSV infection for 24 h. (A) ROS formation was determined by staining with the fluorescent probe DCFHDA. (B-E) The activities of SOD (B), CAT (C), GPx (D), and GST (E) were assessed using specific biochemical assays. Values were presented as mean ± SD of three independent experiments. *P < 0.05 vs. Ctrl group; #P < 0.05 vs. RSV group.

cells. As shown in **Figure 4A**, RSV infection significantly enhanced ROS formation in A549 cells. However, OSC markedly reduced the RSV infection-induced ROS generation. Moreover, we observed a significant reduction in all AOE activities, including SOD (**Figure 4B**), CAT (**Figure 4C**), GPx (**Figure 4D**), and GST (**Figure 4E**) in A549 cells. By contrast, OSC increased the activities of the above-mentioned AOEs. These results demonstrated that OSC inhibits RSV-induced oxidative stress in A549 cells.

OSC-mediated anti-oxidative effects on RSV-infected A549 cells is dependent on Nrf2 activation

Nrf2 is a crucial transcription factor that binds to ARE sequences and regulates expression of antioxidant (e.g., HO-1, NQO-1, SOD, CAT, and GST) and phase II metabolizing enzymes in response to oxidative stress [11]. To investigate the effect of OSC on Nrf2 activation, we detected the protein levels of Nrf2 in the nuclei of RSV-infected A549 cells. **Figure 5A** and **5B** show that nuclear abundance of Nrf2 in RSV-infected A549 cells significantly decreased compared with that in the Ctrl cells. However, this reduction was markedly attenuated by OSC treatment. To confirm the role of Nrf2 in OSC-mediated anti-oxidative effects, we used two siRNAs to knockdown Nrf2 in A549 cells. The siRNA that caused more potent inhibition of

Nrf2 (siNrf2-2) was used in subsequent experiments (**Figure 5C** and **5D**). Nrf2 depletion inhibited the expression of SOD, CAT, and GST in A549 cells infected or uninfected with RSV (**Figure 5E** and **5F**). These results indicated that OSC promotes Nrf2 activation to increase AOE activities in RSV-infected A549 cells.

OSC provides protection against RSV-induced mouse lung injury in vivo

Next, we investigated the potential role of OSC in conferring protection against RSV-induced mouse lung injury. At the indicated time points after RSV infection, the BW of RSV-infected mice significantly decreased compared to that of the Ctrl mice. By contrast, OSC remarkably reduced RSV-induced BW loss (**Figure 6A**). The RSV-infected mice with OSC pretreatment exhibited only mild lung injuries, whereas severe histopathological damages, including fragmentation of alveolar walls and infiltration of lymphocytes, were observed in RSV-treated mice (**Figure 6B** and **6C**). Moreover, lung edema, defined by lung W/D weight ratio, was significantly increased in RSV-infected mice than in Ctrl mice and attenuated by OSC treatment (**Figure 6D**). Consistent with these findings, viral titers were significantly lower in the lung tissue of RSV-infected mice with OSC pretreatment than in RSV-infected mice (**Figure 6E**). OSC pretreatment also considerably
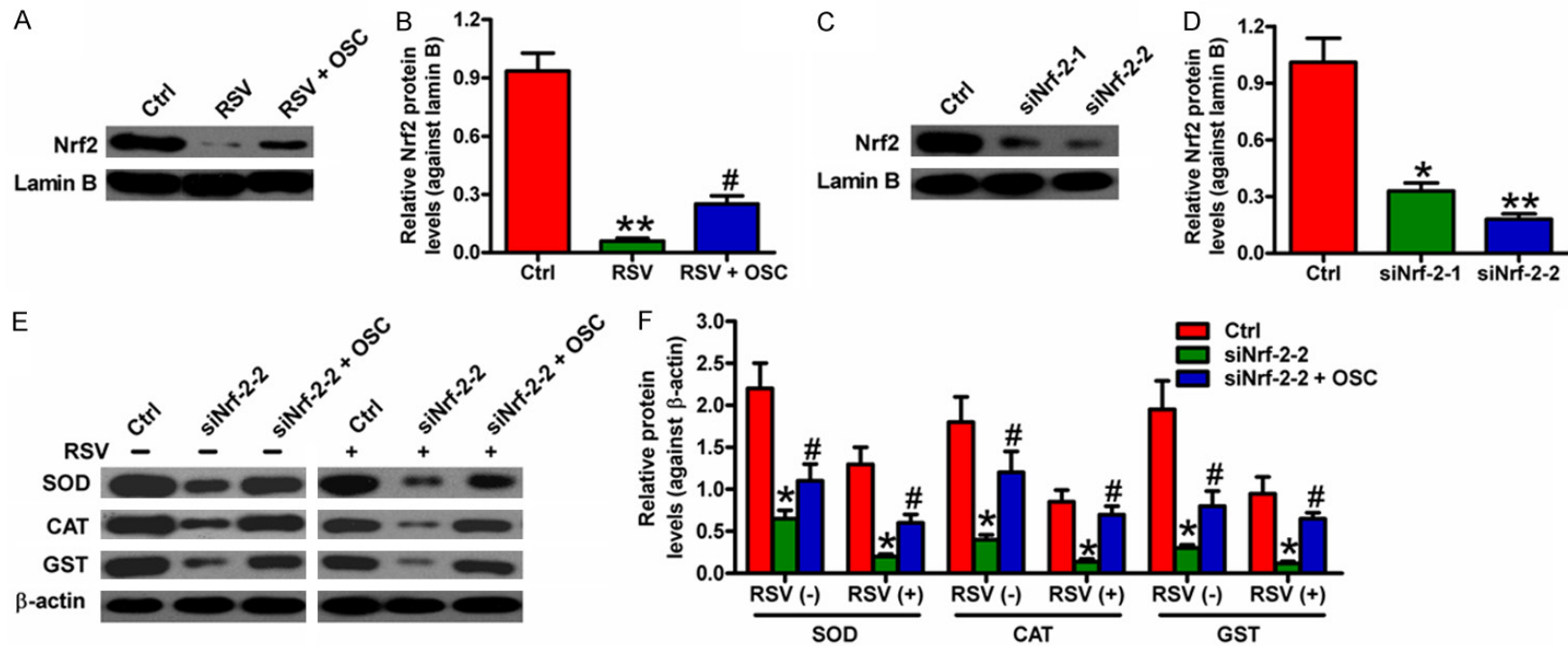
Figure 5. Inhibitory effect of OSC on oxidative stress was mediated by Nrf2 activation in RSV-infected A549 cells. A and B. A549 cells were pretreated with 2 µM of OSC for 1 h followed by 0.3 MOI of RSV infection for 24 h. (A) Nuclear amounts of Nrf2 protein were determined by using Western blot analysis. Lamin B was used as loading control. (B) Quantification of Nrf2 expression in (A). (C and D) A549 cells were transfected with negative control (Ctrl) or siNrf2-1/-2 for 24 h. The expression of Nrf2 was determined by Western blot analysis. (E and F) Ctrl or siNrf2-2-transfected A549 cells were infected with RSV for 24 h. Western blot was performed to detect the expression of SOD, CAT, and GST. Values were presented as mean ± SD of three independent experiments. *$P < 0.05$ vs. Ctrl group; #$P < 0.05$ vs. RSV group.
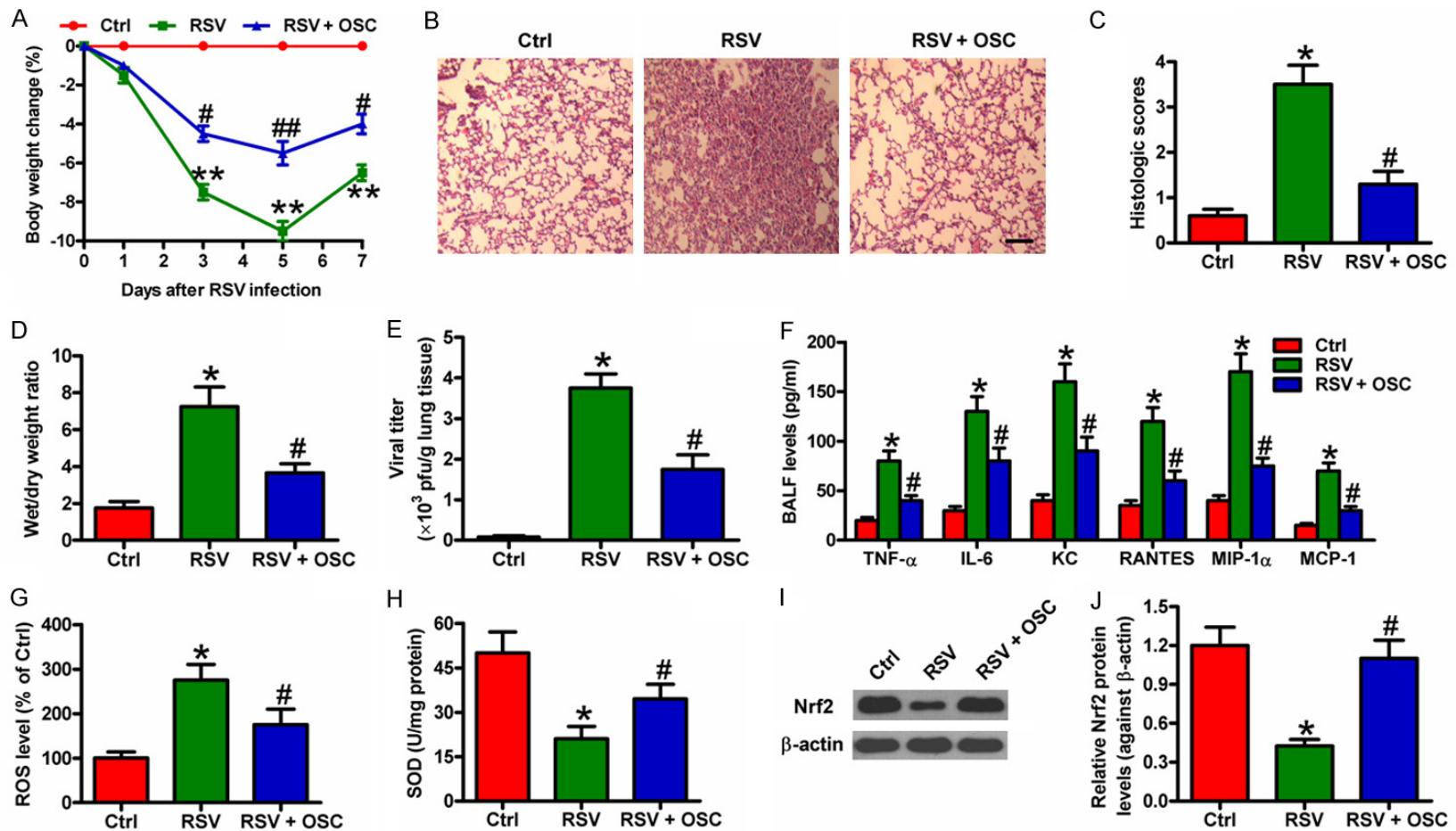
Figure 6. OSC prevented RSV-induced mouse lung injury in vivo. Mice were treated with OSC (80 mg/kg) once daily for 7 days prior to infection with 2×10^7 PFU of RSV. 5 days post-RSV infection, the mice were anesthetized and sacrificed. (A) BW changes were measured once a day. (B) H&E staining of lung sections of the mice 5 days after RSV infection. (C) Score of H&E staining in (B). (D) W/D weight ratio of the mice. (E) Lung viral titers of the mice. (F) Release of pro-inflammatory cytokines and chemokines in the BALFs of mice was measured by ELISAs. (G) ROS production in the lungs of the mice. (H) SOD activity in the lung was assessed using specific biochemical assay. (I and J) Nuclear Nrf2 expression in the lung was detected by Western blot. Values were presented as mean ± SD of three independent experiments. *P < 0.05, **P < 0.01 vs. Ctrl group; #P < 0.05 vs. RSV group.

reduced the release of pro-inflammatory cytokines and chemokines (TNF-α, IL-6, KC, RANTES, MIP-1α, and MCP-1) in the BLAFs of RSV-infected mice (**Figure 6F**). RSV-elevated ROS production in the lung of mice was markedly reduced by OSC treatment (**Figure 6G**), whereas reduction in RSV-induced SOD activity was counteracted by OSC (**Figure 6H**). In addition, OSC promoted Nrf2 activation in the lung of RSV-infected mouse (**Figure 6I** and **6J**). These results suggested that OSC protects against RSV-induced mouse lung injury.

Discussion

In this study, we found that OSC significantly inhibited RSV-induced lung injury in vitro and in vivo. The key findings were as follows. First, OSC reduced RSV replication and improved RSV-infected A549 cell viability. Second, OSC hampered the release of pro-inflammatory cytokines and chemokines in RSV-infected A549 cells. Third, OSC suppressed RSV-induced ROS formation but enhanced AOE activities in A549 cells. Fourth, OSC exerted anti-oxidative effect in RSV-infected A549 cells in an Nrf2-dependent manner. Last, the protective effects of OSC against RSV-induced mouse lung injury in vivo were highly consistent with the findings in vitro.

Previous studies have shown that pro-inflammatory cytokines and chemokines are produced during RSV infection, which play a central role in the pathogenesis of RSV-induced lung disease [27]. These effects have been associated to the activation of mitogen-activated protein kinase and transcription factor nuclear factor-κB, which are responsible for the transcription of inflammatory mediators [28]. Here, we found that OSC treatment partially increased the viability of RSV-infected A549 cells and markedly reduced RSV-induced production of pro-inflammatory cytokines and chemokines in vitro and in vivo, suggesting that OSC exerted anti-inflammatory effect on RSV-induced lung injury.

Oxidative stress has been implicated in the pathogenesis of several acute and chronic airway diseases, such as asthma and chronic obstructive pulmonary disease [29]. ROS can be induced by a variety of stimulators and certain viruses, such as influenza, hepatitis B, rhinovirus, and HIV [30]. Specifically, studies have

shown that RSV infection induces ROS production in airway epithelial cells and that inhibition of ROS generation by antioxidant administration significantly blocks transcription factor activation and chemokine gene expression in vitro [6, 7], as well as ameliorates RSV-induced lung injury in vivo [24]. Moreover, the expression and activity of AOEs involved in maintaining cellular oxidant/antioxidant balance were reduced by RSV infection in vitro and in vivo [8, 9, 24]. The present study demonstrated that RSV increased ROS formation and reduced AOE activities in vitro and in vivo, which were reversed by OSC treatment.

AOE genes were transcribed by Nrf2 by its binding to the ARE site located in promoters [10]. Several viruses, such as hepatitis B and C viruses and human cytomegalovirus, induce ARE-dependent responses by activating Nrf2 [31-33]. A recent study has shown that the Nrf2-ARE pathway plays a protective role against RSV-induced injury and oxidative stress in murine airways [16]. Komaravelli et al. [34] demonstrated that RSV infection induces a progressive reduction in nuclear and total cellular levels of Nrf2, resulting in reduced binding to the AOE gene promoters and decreased AOE expression. Pretreatment with an Nrf2 inducer significantly limited lung RSV replication and RSV-induced inflammation in Nrf2^{+/+} but not in Nrf2^{-/-} mice, suggesting the antiviral activity of Nrf2 in a mouse model of RSV disease [16]. This study showed that Nrf2 in nuclei was reduced in RSV-infected A549 cells and mouse lung; however, OSC attenuated this reduction, suggesting that the anti-oxidative effect of OSC on RSV-induced lung damage in vitro and in vivo was dependent on Nrf2 activation.

In summary, OSC is a potential suppressor of lung inflammation and oxidative stress associated with RSV infection in vitro and in vivo. We found that OSC reduces the RSV-induced lung injury by activating Nrf2-ARE signaling pathway, suggesting the beneficial effects in prevention of RSV infection and/or reduction of severity of RSV-induced lung disease.

Disclosure of conflict of interest

None.

Address correspondence to: Jie Gao, Department of Pediatrics, Henan University Huaihe Hospital,

115 Ximen Street, Kaifeng 475000, Henan, P. R. China. Tel: 86-371-23906557; Fax: 86-371-2390-6557; E-mail: jiegaokf@sohu.com

References

[1]   van Woensel JB, van Aalderen WM and Kimpen JL. Viral lower respiratory tract infection in infants and young children. BMJ 2003; 327: 36-40.

[2]   Falsey AR. Respiratory syncytial virus infection in elderly and high-risk adults. Exp Lung Res 2005; 31 Suppl 1: 77.

[3]   Papin JF, Wolf RF, Kosanke SD, Jenkins JD, Moore SN, Anderson MP and Welliver RC Sr. Infant baboons infected with respiratory syncytial virus develop clinical and pathological changes that parallel those of human infants. Am J Physiol Lung Cell Mol Physiol 2013; 304: L530-539.

[4]   Garofalo RP and Haeberle H. Epithelial regulation of innate immunity to respiratory syncytial virus. Am J Respir Cell Mol Biol 2000; 23: 581-585.

[5]   MacNee W. Oxidative stress and lung inflammation in airways disease. Eur J Pharmacol 2001; 429: 195-207.

[6]   Casola A, Burger N, Liu T, Jamaluddin M, Brasier AR and Garofalo RP. Oxidant tone regulates RANTES gene expression in airway epithelial cells infected with respiratory syncytial virus. Role in viral-induced interferon regulatory factor activation. J Biol Chem 2001; 276: 19715-19722.

[7]   Liu T, Castro S, Brasier AR, Jamaluddin M, Garofalo RP and Casola A. Reactive oxygen species mediate virus-induced STAT activation: role of tyrosine phosphatases. J Biol Chem 2004; 279: 2461-2469.

[8]   Hosakote YM, Liu T, Castro SM, Garofalo RP and Casola A. Respiratory syncytial virus induces oxidative stress by modulating antioxidant enzymes. Am J Respir Cell Mol Biol 2009; 41: 348-357.

[9]   Hosakote YM, Jantzi PD, Esham DL, Spratt H, Kurosky A, Casola A and Garofalo RP. Viral-mediated inhibition of antioxidant enzymes contributes to the pathogenesis of severe respiratory syncytial virus bronchiolitis. Am J Respir Crit Care Med 2011; 183: 1550-1560.

[10]   Jaiswal AK. Nrf2 signaling in coordinated activation of antioxidant gene expression. Free Radic Biol Med 2004; 36: 1199-1207.

[11]   Kaspar JW, Niture SK and Jaiswal AK. Nrf2: INrf2 (Keap1) signaling in oxidative stress. Free Radic Biol Med 2009; 47: 1304-1309.

[12]   Cho HY, Jedlicka AE, Reddy SP, Kensler TW, Yamamoto M, Zhang LY and Kleeberger SR. Role of NRF2 in protection against hyperoxic lung injury in mice. Am J Respir Cell Mol Biol 2002; 26: 175-182.

[13]   Rangasamy T, Cho CY, Thimmulappa RK, Zhen L, Srisuma SS, Kensler TW, Yamamoto M, Petrache I, Tuder RM and Biswal S. Genetic ablation of Nrf2 enhances susceptibility to cigarette smoke-induced emphysema in mice. J Clin Invest 2004; 114: 1248-1259.

[14]   Cho HY, Reddy SP, Yamamoto M and Kleeberger SR. The transcription factor NRF2 protects against pulmonary fibrosis. FASEB J 2004; 18: 1258-1260.

[15]   Rangasamy T, Guo J, Mitzner WA, Roman J, Singh A, Fryer AD, Yamamoto M, Kensler TW, Tuder RM, Georas SN and Biswal S. Disruption of Nrf2 enhances susceptibility to severe airway inflammation and asthma in mice. J Exp Med 2005; 202: 47-59.

[16]   Cho HY, Imani F, Miller-DeGraff L, Walters D, Melendi GA, Yamamoto M, Polack FP and Kleeberger SR. Antiviral activity of Nrf2 in a murine model of respiratory syncytial virus disease. Am J Respir Crit Care Med 2009; 179: 138-150.

[17]   Zhu QL, Li YX, Zhou R, Ma NT, Chang RY, Wang TF, Zhang Y, Chen XP, Hao YJ, Jin SJ, Ma L, Du J, Sun T and Yu JQ. Neuroprotective effects of oxysophocarpine on neonatal rat primary cultured hippocampal neurons injured by oxygen-glucose deprivation and reperfusion. Pharm Biol 2014; 52: 1052-1059.

[18]   Yang Y, Li YX, Wang HL, Jin SJ, Zhou R, Qiao HQ, Du J, Wu J, Zhao CJ, Niu Y, Sun T and Yu JQ. Oxysophocarpine Ameliorates Carrageenan-induced Inflammatory Pain via Inhibiting Expressions of Prostaglandin E2 and Cytokines in Mice. Planta Med 2015; 81: 791-797.

[19]   Xu T, Li Y, Wang H, Xu Y, Ma L, Sun T, Ma H and Yu J. Oxysophocarpine induces anti-nociception and increases the expression of GABAAalpha1 receptors in mice. Mol Med Rep 2013; 7: 1819-1825.

[20]   Pan QM, Li YH, Hua J, Huang FP, Wang HS and Liang D. Antiviral Matrine-Type Alkaloids from the Rhizomes of Sophora tonkinensis. J Nat Prod 2015; 78: 1683-1688.

[21]   Ding PL, Liao ZX, Huang H, Zhou P and Chen DF. (+)-12alpha-Hydroxysophocarpine, a new quinolizidine alkaloid and related anti-HBV alkaloids from Sophora flavescens. Bioorg Med Chem Lett 2006; 16: 1231-1235.

[22]   Yang Y, Guan F, Bai L, Zhang L, Liu J, Pan X and Zhang L. Quinolizidine alkaloids reduced mortality in EV71-infected mice by compensating for the levels of T cells. Bioorg Med Chem Lett 2015; 25: 3526-3528.

[23]   Ueba O. Respiratory syncytial virus. I. Concentration and purification of the infectious virus. Acta Med Okayama 1978; 32: 265-272.

[24] Castro SM, Guerrero-Plata A, Suarez-Real G, Adegboyega PA, Colasurdo GN, Khan AM, Garofalo RP and Casola A. Antioxidant treatment ameliorates respiratory syncytial virus-induced disease and lung inflammation. Am J Respir Crit Care Med 2006; 174: 1361-1369.

[25] Matrosovich M, Matrosovich T, Garten W and Klenk HD. New low-viscosity overlay medium for viral plaque assays. Virol J 2006; 3: 63.

[26] Collins PL and Graham BS. Viral and host factors in human respiratory syncytial virus pathogenesis. J Virol 2008; 82: 2040-2055.

[27] Zeng R, Li C, Li N, Wei L and Cui Y. The role of cytokines and chemokines in severe respiratory syncytial virus infection and subsequent asthma. Cytokine 2011; 53: 1-7.

[28] Allen RG and Tresini M. Oxidative stress and gene regulation. Free Radic Biol Med 2000; 28: 463-499.

[29] Folkerts G, Kloek J, Muijsers RB and Nijkamp FP. Reactive nitrogen and oxygen species in airway inflammation. Eur J Pharmacol 2001; 429: 251-262.

[30] Schwarz KB. Oxidative stress during viral infection: a review. Free Radic Biol Med 1996; 21: 641-649.

[31] Schaedler S, Krause J, Himmelsbach K, Carvajal-Yepes M, Lieder F, Klingel K, Nassal M, Weiss TS, Werner S and Hildt E. Hepatitis B virus induces expression of antioxidant response element-regulated genes by activation of Nrf2. J Biol Chem 2010; 285: 41074-41086.

[32] Burdette D, Olivarez M and Waris G. Activation of transcription factor Nrf2 by hepatitis C virus induces the cell-survival pathway. J Gen Virol 2010; 91: 681-690.

[33] Lee J, Koh K, Kim YE, Ahn JH and Kim S. Upregulation of Nrf2 expression by human cytomegalovirus infection protects host cells from oxidative stress. J Gen Virol 2013; 94: 1658-1668.

[34] Komaravelli N, Tian B, Ivanciuc T, Mautemps N, Brasier AR, Garofalo RP and Casola A. Respiratory syncytial virus infection down-regulates antioxidant enzyme expression by triggering deacetylation-proteasomal degradation of Nrf2. Free Radic Biol Med 2015; 88: 391-403.